27th ABCM International Congress of Mechanical Engineering
December 04-08, 2023, Florianópolis-SC, Brazil

COB-2023-1662
MODELING AND VALIDATION OF THE LONGITUDINAL DYNAMICS OF A 2WD VEHICLE WITH MECHANICALLY DRIVEN CVT

Rodrigo Souza Nunes da Silva
Guilherme Warwick Parker Maia
Bruno José Abad Miranda Silva
Gabriel Batista Macedo
Caio Beltrão Moraes Rolemberg
André de Souza Mendes
Centro Universitário FEI. Av. Humberto de Alencar Castelo Branco, 3972 - Assunção, São Bernardo do Campo - SP
rodrigosouza.n.d.s@gmail.com; gwparkermaia@gmail.com; bj-abad@hotmail.com; gbmacedo08@gmail.com; caio.rolemberg@hotmail.com; asmendes@fei.edu.br

Abstract. *The use of simulators and fully digital models are increasingly used in engineering to develop and evaluate diverse experimental projects. The benefits of simulation models are evident, for instance, in the development of vehicles with mechanically driven continuously variable transmission (CVT). Obtaining these vehicle setups through purely practical means is usually prohibitive, considering the time, material, and high labor required to achieve this. Therefore, this research uses MATLAB software to develop and validate a computational model of the longitudinal dynamics of a 2WD vehicle equipped with a mechanically driven CVT transmission. With this model, it is possible to reduce the cost and time of development and tuning of the CVT. The FEI Baja 2WD prototype is used in this research, whose design criteria are based on the Baja SAE BRASIL competition. This research is divided into three major parts: model development, vehicle data collection, and model validation. Regarding model development, MATLAB/SIMULINK is used to create the simulation model of the system that includes the dynamics of the CVT transmission and the longitudinal dynamics of the vehicle. Regarding data collection and validation, the setup's performance is assessed through the vehicle acceleration with wide-open throttle and measuring engine RPM and the rotational speed of the driving wheels. Evaluating the model's performance in predicting the real vehicle behavior allows for verifying where divergences occur, indicating improvement points, and developing methods to validate the model. This paper presents a preliminary result using the current version of the proposed model with good agreement between the experimental and simulated results.*

Keywords: *Modeling, Validation, Longitudinal dynamics, CVT, BAJA SAE, MATLAB, SIMULINK.*

1. INTRODUCTION

Due to growing environmental concerns, rising fuel prices, and government regulations on gas emissions, energy efficiency requirements for machines are becoming increasingly stringent. Therefore, energy efficiency is a critical parameter and must comply with government laws and regulations, in addition to meeting the requirements of the end consumer (Srivastava and Haque, 2009).

Engineering projects must meet increasingly stringent requirements for energy efficiency and performance. Achieving these goals requires the integration of advanced computational methods in engineering processes. By harnessing computational advances in engineering areas, it becomes possible to streamline the design validation and system optimization processes, leading to significant cost and labor reductions (Julió and Plante, 2011).

In a broad sense, energy efficiency refers to how much energy is effectively used for the desired purpose. In the context of mechanical transmission systems, energy efficiency is particularly relevant, as it indicates whether the mechanical energy generated by the engine is being transmitted efficiently to the other components of the system. Factors such as frictional losses and inefficiencies in coupling interfaces can influence energy efficiency in mechanical transmission systems (Arango and Alzate, 2020).

Mechanical transmission plays a crucial role in a vehicle's efficiency in terms of performance and fuel economy and encompasses many types and configurations. There are two main types of transmissions: manual transmission and automatic transmission. The Continuously Variable Transmission (CVT) is a type of automatic transmission that does not have traditional gears like a conventional automatic transmission. Instead, it uses a system of variable radius pulleys and belts or chains to provide a continuous range of gear ratios. In this way, the CVT transmission can offer a wide range of gear ratios, allowing the engine to run without interrupting the torque delivered to the vehicle's wheels and in its most efficient RPM range under different driving conditions. This system is used in vehicles like cars, All Terrain Vehicle (ATV), Snowmobile, trucks, and vans (Ding, Zhu, and Liu, 2011).

Figure 1 - FEI Baja 2WD prototype (Left) and the CVT transmission (Right) used in this research.

Tuning a mechanically driven continuously variable transmission (CVT) can be a complex process that requires expertise and specialized knowledge (Skinner, 2020). It is generally more challenging to tune a CVT than other transmissions, such as conventional automatic or manual transmissions. The complexity arises from the intricate interaction between various components in the CVT system, including the pulleys, belts, and flyweight mechanisms. Therefore, this article aims to develop and experimentally validate a mathematical model of the longitudinal dynamics of a vehicle equipped with a flyweight CVT transmission and rubber belt using SIMULINK/MATLAB software. The FEI Baja 2WD prototype is used in this research. This computational model will reduce the time and cost of experimental tests for tuning the transmission under different operating conditions.

2. LITERATURE REVIEW

Many authors have studied the development of virtual models to represent the operation of mechanical CVTs, such as Arango and Azalte (2020), Willis (2006), and Skinner (2020). Arango and Azalte (2020) address this issue by developing longitudinal dynamics equations coupled to V-pulley equations for belt stress calculation. Its equations transform the axial force to torque as a function of friction, kinematics of the primary pulley, and forces on the two pulleys, resulting in data consistent with the expected results, demonstrating the possibility of implementing virtual systems in educational engineering projects. A different method is used by Willis (2006). Its equations are developed considering energy balances in both pulleys and kinematic principles to describe the primary pulley's movement. This method can reduce the tuning time after the car's construction and optimize the prototype's performance. The software proposed by the authors requests the desired working rotations for the CVT and provides the parameters of the two pulleys necessary for its operation. Skinner (2020) developed a test bench with a water brake dynamometer and hall sensors, monitoring the engine's torque and the variation of the ratio of the pulleys as a function of the engine's rotation. With this data, the behavior of the CVT is described more accurately by considering the force balance between the pulleys, the torque input of the engine, external loads, and the centrifugal force of the belt.

Lolli et al. (2003) describe the power transmission by rubber belts analytically, studying how the axial forces of the pulleys result in radial forces on the belt, then describing the calculation of the friction coefficient. This analytical description uses a finite element method with parameters obtained in a test bench developed by the author. Furthermore, a method of evaluating the estimated life of V-belts applied to CVTs was developed, comparing the failures in the belts obtained experimentally with those obtained by the software.

The relation between the rotation of the pulleys of a CVT and its geometric radii (slip) is one of the most crucial factors to consider for efficient power transmission in CVTs. Therefore, Bonsen et al. (2003) describe the slip as a function of the axial force in the pulleys, developing a control model to study the necessary axial actuation using a hydraulic system in the primary pulley. Moreover, the authors study the influence of the geometric ratio between the pulleys, the traction coefficient, and the transmission efficiency on the slip.

Julió and Plante (2011) proposed an analytical model in which the primary pulley's axial force and rotation and the secondary pulley's resistive torque are used as input parameters. The authors discretize the belt as nodes connected by springs, evaluating different friction models for the belt-pulley contact. With this, the primary pulley's kinematic description and the secondary pulley's forces are developed and compared with results obtained from a test bench with the electronically controlled primary pulley.

As a simplified analysis of the operation of a CVT, Anderson (2017) models its behavior as a steady-state phenomenon, performing a quasi-static analysis, disregarding all accelerations, except for centripetal ones, and considering a balance between the forces of the primary pulley and secondary pulley. For this, the kinematics of the flyweight arms are considered, together with the forces of the springs and the secondary pulley cam.

Mechanical CVTs are devices that involve a series of interdependent variables, whose appropriate combination is responsible for their optimal performance. Khan and Dhongde (2014) proposed a model that establishes a mathematical correlation between these variables that influence CVT performance and efficiency to create a logical control of the CVT ratio according to the road load demand. For this, the characteristics of the secondary and primary pulley springs, ramp profile, masses, and helix cam were considered. Then, the mechanism responsible for generating the clamping force on the belt was modified to allow electronic control. The electronic control was validated on dynamometers, demonstrating a reduction in fuel consumption and an improvement in acceleration.

The primary pulley ramp profile is an important part of the CVT, directly affecting its operation and the vehicle's behavior. Thus, Ding, Zhu, and Liu (2011) studied the influence of the ramp profile composed of several arcs using a numerical model of the rubber V-belt in steady-state. This way, it was possible to obtain an ideal arc profile, considering the behavior of the CVT and a constant engine speed at peak power during the variation of the pulley’s ratio.

An alternative approach is proposed by Aulakh (2017), in which the author develops a simulation model using Genetic Algorithms (GA) to optimize the fit of a transmitted continuous variable (CVT). In this study, a mathematical model of the CVT is implemented in the MATLAB programming environment. A two-level GA controls the CVT variables and obtains the desired behavior, including appropriate engagement at maximum engine torque and the beginning of the shift-out phase at maximum engine power, maintaining this speed until the final ratio. Through this process, the developed model calculates the profile angles of the ramp and the cam, the characteristics of the primary and secondary pulleys' springs, and the mass necessary to achieve the desired behavior. The developed model was validated.

Gangadurai, Harikrishnan, and Sreekumar (2005) introduce an enhanced design concept for a continuously variable transmission (CVT). The primary goal of the research is to gain a comprehensive understanding of the working principles of CVT transmission. To achieve this, the authors conduct experimental tests and develop a mathematical model of the CVT transmission using MATLAB. The model is then validated with the experimental data to ensure its accuracy. The authors leverage the validated mathematical model to determine the ideal parameter values necessary for the CVT's proper operation.

Previous work generally addresses the mathematical model development, experimental validation, and different applications of CVT models to increase efficiency and performance. The present article aims to contribute to the former two objectives.

3. METHODS

This section presents the mathematical models, computational model and determination of parameters for the experimental validation test.

3.1 Mathematical models

The mathematical models must characterize the vehicle's longitudinal dynamics and flyweight-type CVT dynamics to reproduce the typical behavior of an accelerating vehicle equipped with a CVT transmission: clutching phase, low ratio acceleration, shift point, and high ratio acceleration (Aaen, 2015).

3.1.1 Longitudinal dynamics

The longitudinal dynamics of the vehicle is described by the differential equation (1).

$$(m + m_e)a = F_x - D_A - R_x - W \sin\theta \quad (1)$$

where m is the mass of the vehicle and driver, m_e the equivalent mass of the rotating components, a the longitudinal acceleration, F_x the tractive force, D_A the aerodynamic drag force, R_x the rolling resistance force, W the weight force of the vehicle and θ the road slope.

The rolling resistance force is

$$R_x = C_{r1}v + C_{r0} \quad (2)$$

where C_{r1} and C_{r0} are the constants of the linear model.

The aerodynamic drag is characterized by the equation (3).

$$D_A = \frac{1}{2}\rho C_D A v^2 \tag{3}$$

where ρ is the air density, C_D the aerodynamic drag coefficient, A the frontal area of the vehicle and v the vehicle speed.

The longitudinal dynamics depends on the current phase of the acceleration. Traction force is generated according to the acceleration phase, clutching and fully engaged, explained in the following sections. The torque generated by the engine over a throttle input is modeled as a first-order dynamics with a 0.05 s time constant.

3.1.2 Traction force during clutching phase

During the clutching phase, the torque is transmitted by means of friction between the belt and the pulleys. The engine dynamics is given by (Bonsen et al, 2005)

$$\dot{\omega}_e = \frac{T_e - T_p}{(I_e + I_p)} \tag{4}$$

where I_e is the moment of inertia of the engine and I_p is the moment of inertia of the primary pulley set. T_e is the engine torque and T_p is the torque transmitted by the primary pulley and is defined as

$$T_p = \frac{2F_p R_p \mu}{\cos\alpha} \tag{5}$$

where F_p is the primary clamping force, R_p is the running radius on the primary pulley. The friction coefficient is μ and the pulley wedge angle is α.

The torque transmitted by the secondary pulley is

$$T_s = N_g T_p \tag{6}$$

where N_g is the CVT geometric ratio

$$N_g = \frac{R_s}{R_p} \tag{7}$$

Thus, the tractive force is

$$F_x = \frac{T_s N_f}{r} \tag{8}$$

where N_f is the gearbox ratio and r is the wheel radius.

The relative slip between belt and pulleys is defined as

$$\nu = 1 - \frac{r_s}{r_g} \tag{9}$$

where the speed and geometric ratios are

$$r_s = \frac{\omega_s}{\omega_p} \tag{10}$$

$$r_g = \frac{R_p}{R_s} \tag{11}$$

respectively.

The clutching phase lasts until the relative slip ν is zero. In this phase, the equivalent mass of the rotating components m_e accounts only for the rotating elements from the secondary pulley up to the driving wheels.

3.1.3 Traction force during fully engaged phase

Since no slip occurs when the CVT transmission is fully engaged, the tractive force is characterized by the equation (12).

$$F_x = \frac{T_e N_g N_f}{r} \tag{12}$$

In this case, the equivalent mass of the rotating components m_e accounts for all the rotating elements from the drivetrain.

3.1.4 Sheaves dynamics

The CVT transmission ratio will change based on the dynamics of the pulley sheaves. The dynamics of the CVT introduces an additional degree of freedom to the model. Figure 2 illustrate the mechanics of the primary and secondary pulleys and the main acting forces.

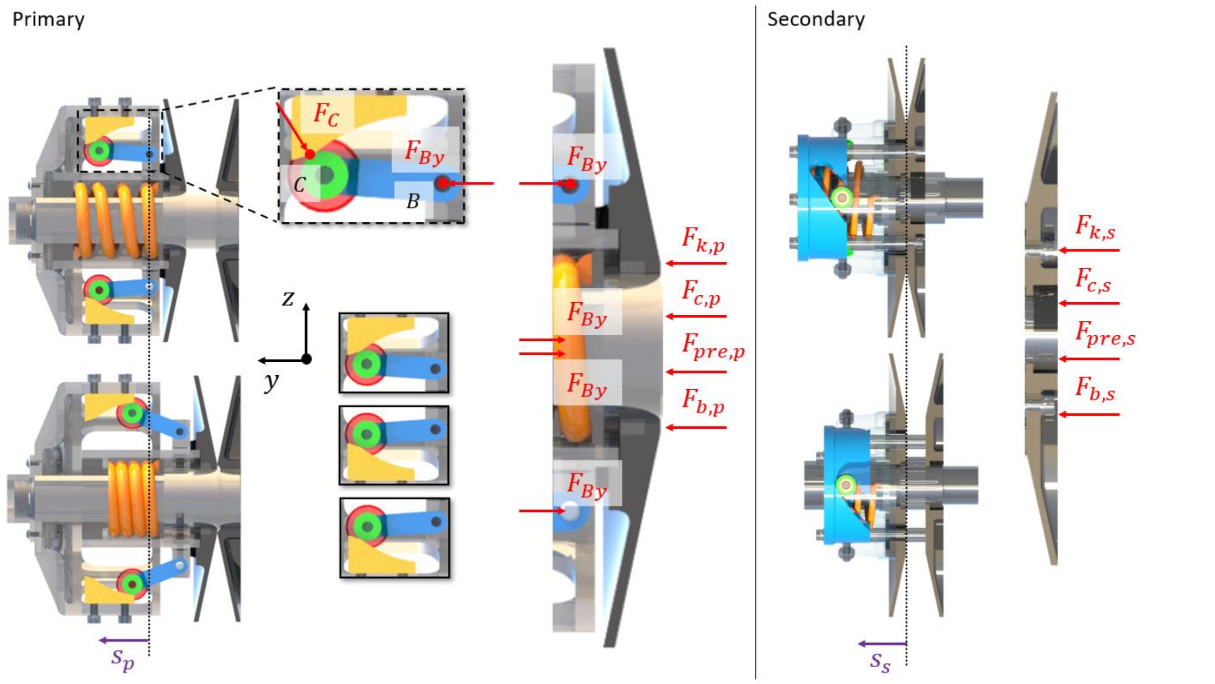

Figure 2 – Primary (left) and secondary (right) pulleys and the forces acting on each movable sheave.

The axial dynamics of the primary pulley is

$$m_p \ddot{s}_p = -4F_{By} + F_{k,p} + F_{c,p} + F_{pre,p} + F_{b,p} \tag{13}$$

where m_p is the mass of all elements moving axially. $F_{b,p}$ is the axial force performed by the belt on the movable sheave of the primary pulley. $F_{pre,p}$ is the preload in the primary pulley, assumed constant.

The stiffness and damping forces in this direction are defined as

$$F_{k,p} = -k_p s_p \tag{14}$$
$$F_{c,p} = -c_p \dot{s}_p \tag{15}$$

where k_p and c_p are the stiffness and damping coefficients of the primary sheave, respectively. The axial position, speed and acceleration of the set are s_p, $\dot{s}_p$, $\ddot{s}_p$, respectively. F_{By} is the axial force generated by each of the four flyweights rolling against the ramp because of the centrifugal force. In this model, the ramp is modeled as a two-section ramp. As seen in Figure 2, the first section presents a constant slope. Although the second section presents a variable slope ramp, for simplicity, the second section is modeled as a constant slope as well.

The axial dynamics of the secondary pulley is

$$m_s \ddot{s}_s = F_{k,s} + F_{c,s} + F_{pre,s} + F_{b,s} \tag{16}$$

where m_s is the mass of all elements from the secondary pulley moving axially. $F_{b,s}$ is the axial force performed by the belt on the movable sheave of the secondary pulley. $F_{pre,s}$ is the preload in the secondary, defined as

$$F_{pre,s} = F_{pre,s,0} + 0{,}225(T_e N_g)/(2r_h \tan\beta) \tag{17}$$

where $F_{pre,s,0}$ is a constant preload value and the last addend accounts for the variable part of the preload, where r_h and β are the radius and angle of the helix, respectively.

The stiffness and damping forces in this direction are defined as

$$F_{k,s} = -k_s s_s \tag{18}$$
$$F_{c,s} = -c_s \dot{s}_s \tag{19}$$

where k_s and c_s are the stiffness and damping coefficients of the secondary sheave, respectively. The axial position, speed and acceleration of the secondary sheave are s_p, $\dot{s}_p$, $\ddot{s}_p$, respectively. Both dynamics are constraint by the length of the belt, resulting in only one additional degree of freedom.

Assuming a linear relationship between the displacements of the sheaves, i.e.,

$$s_s = h_{ps} s_p \tag{20}$$

the resulting dynamics based on the displacement of the primary sheave is

$$\ddot{s}_p = \left(-4F_{By} - \left(k_p + h_{ps}^2 k_s\right)s_p - \left(c_p + h_{ps}^2 c_s\right)\dot{s}_p + F_{pre,p} + F_{pre,s}\right)/(m_p + h_{ps}^2 m_s) \tag{21}$$

3.2 Computational model

The mathematical model described in section 3.1 is computationally implemented in the SIMULINK feature of MATLAB software. The framework of the simulator is illustrated in Figure 3. The model's only input is the throttle position, and the main output is the longitudinal speed of the vehicle. The other variables of interest are accessible in the diagram. A structure of three subsystems is implemented: Engine, CVT transmission, and longitudinal dynamics.

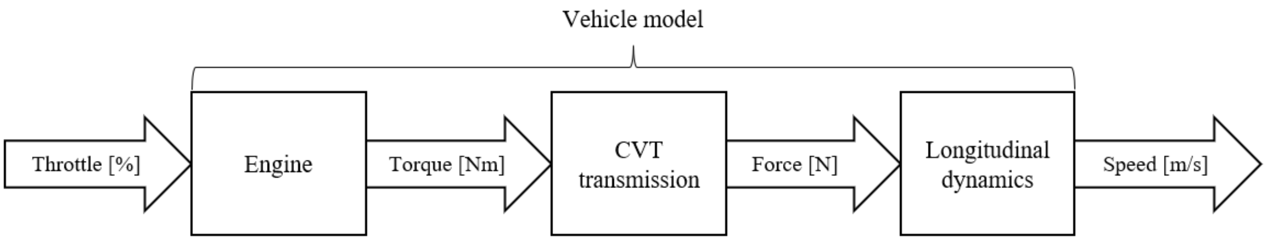

Figure 3 - Simulation framework in SIMULINK. Throttle is the input, and the main output is the speed of the vehicle.

The Engine block takes as input the throttle position and, with the current rotational speed of the engine, generates the engine torque signal based on the wide-open throttle torque curve. The engine torque is fed to the CVT transmission subsystem, where the dynamics of the sheaves are implemented using MATLAB Functions, and the traction force signal is generated according to the acceleration phase (Sections 3.1.2 and 3.1.3). The traction force is fed to the Longitudinal dynamics block, where the longitudinal kinematics are obtained, for instance, position, speed, and acceleration.

3.3 Parameters

A Briggs & Stratton 10 hp engine is used in this research. The torque curve of this engine is illustrated in Figure 4.

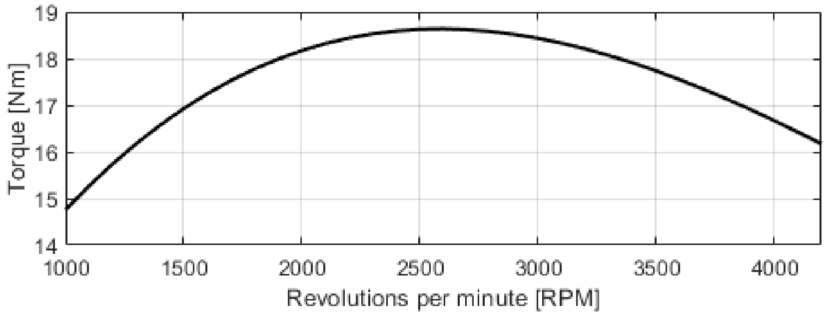

Figure 4 – Torque curve of the Briggs & Stratton 10 hp engine.

The elastic coefficients of the springs were obtained using the results of a Tensile Testing Machine (MTS). With the applied load and the press displacement value, which is equivalent to the spring deformation, we can calculate the elastic coefficient value according to Hooke's Law (linear model).

The spring of the primary pulley has a linear behavior and therefore was positioned directly on the MTS, as shown in the left picture in Figure 5. Since the spring used in the secondary pulley undergoes torsion and compression simultaneously, a special device (central picture in Figure 5) was developed to allow translation and rotation of the sheave guided by the angled cam (right picture in Figure 5). The springs used in the secondary pulley present a linear behavior for a given preload during its operation. To obtain the values of equivalent elastic coefficients and preloads, trend lines are fitted to the data provided by the MTS.

Figure 5 - On the left, the primary pulley spring on the MTS. In the center, the special device used for the secondary pulley. On the right, the secondary pulley with the special device on the MTS.

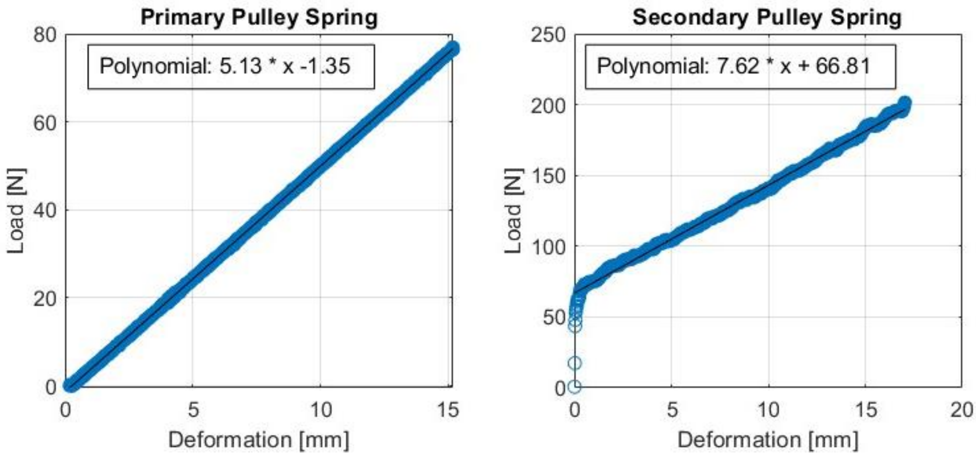

Figure 6 -. Results obtained with the MTS test.

3.4 Sensors

Two speed sensors are used to collect the data in this system. The first is positioned on the motor shaft. A phonic wheel is used to determine the speed of the motor. This measurement allows us to determine the speed of the primary pulley. The second sensor is placed in the reduction box. The speed of the secondary pulley ω_s and the speed of the vehicle v are calculated as

$$\omega_s = N_f \omega_w \tag{22}$$
$$v = r\omega_w \tag{23}$$

where ω_w is the rotational speed of the rear wheel.

The sensors and the module communicate through a Controller Area Network (CAN). The data is stored in AIM EVO 5 and later retrieved for analysis. Then, the RACE STUDIO 3 software is used to perform data interpretation. In the software, the collected data are used to plot graphs and to identify the phases of operation of the CVT.

4. RESULTS

Data collection took place during a test session performed on a flat horizontal straight road. The car accelerates from a stationary position maintaining full throttle.

Table 1 - Main parameters of the vehicle and the CVT.

Parameter	Description	Value	Unit
A	Frontal area projection.	1.14	m²
α	Pulley wedge angle.	0.22	rad
β	Helix angle of the secondary pulley.	0.61	rad
C_d	Aerodynamic drag coefficient.	1.04	-
$F_{pre,p}$	Primary pulley spring preload.	400.00	N
$F_{pre,s}$	Secondary pulley spring preload.	66.00	N
g	Acceleration of gravity.	9.81	m/s²
k_p	Stiffness of the primary pulley spring.	5130.00	Nm
k_s	Stiffness of the secondary pulley spring.	7620.00	Nm
L	Belt length.	1.37	m
m	Mass of the vehicle with pilot.	220.00	kg
m_C	Mass of the flyweights.	0.125	kg
r	Dynamic wheel radius.	0.27	m
r_h	Helix radius of the secondary pulley	0.041	m
$R_{p,max}$	Maximum radius of the primary pulley.	0.071	m
$R_{p,min}$	Minimum radius of the primary pulley.	0.027	m
$R_{s,max}$	Maximum radius of the secondary pulley.	0.097	m
$R_{s,min}$	Minimum radius of the secondary pulley.	0.059	m
ρ	Air density.	1.225	kg/m³
X	Distance of shaft centers between primary and secondary pulleys.	0.254	m

The experimental and simulated results are illustrated in Figure 8. The three main signals representing the longitudinal dynamics are illustrated over time: longitudinal speed, engine RPM, and speed ratio. The experimental result is presented in the three graphs with the responses of the computational model proposed in this article. It is possible to observe that the simulated result is composed of the clutching phase, when slip occurs between the belt and the pulleys, and the fully engaged phase, when there is no slip and the geometric relationship of the pulley radii coincides with the speed ratio of the pulleys.

At the start of the simulation, a step input is applied to the accelerator pedal, and the engine speed rises. At instant 0.3 s, the clutching phase starts. The secondary pulley is activated and starts to rotate, changing the speed ratio and moving the vehicle. During this phase, engine torque is transferred by the CVT with some level of slip between the primary pulley and the belt. The clutching phase ends at 0.9 s, with the engine turning at approximately 2600 RPM. From this point on, there is no more slippage. Between instants 0.9 s and 1.6 s, the car's speed increases according to the low ratio CVT (r_s=0.27). At instant 1.6 s, the shift-out point is reached with the engine speed at approximately 4000 RPM, and the CVT geometric ratio changes. The car accelerates while the CVT ratio goes from r_s=0.27 to r_s=0.66 at the end of the acquisition time series.

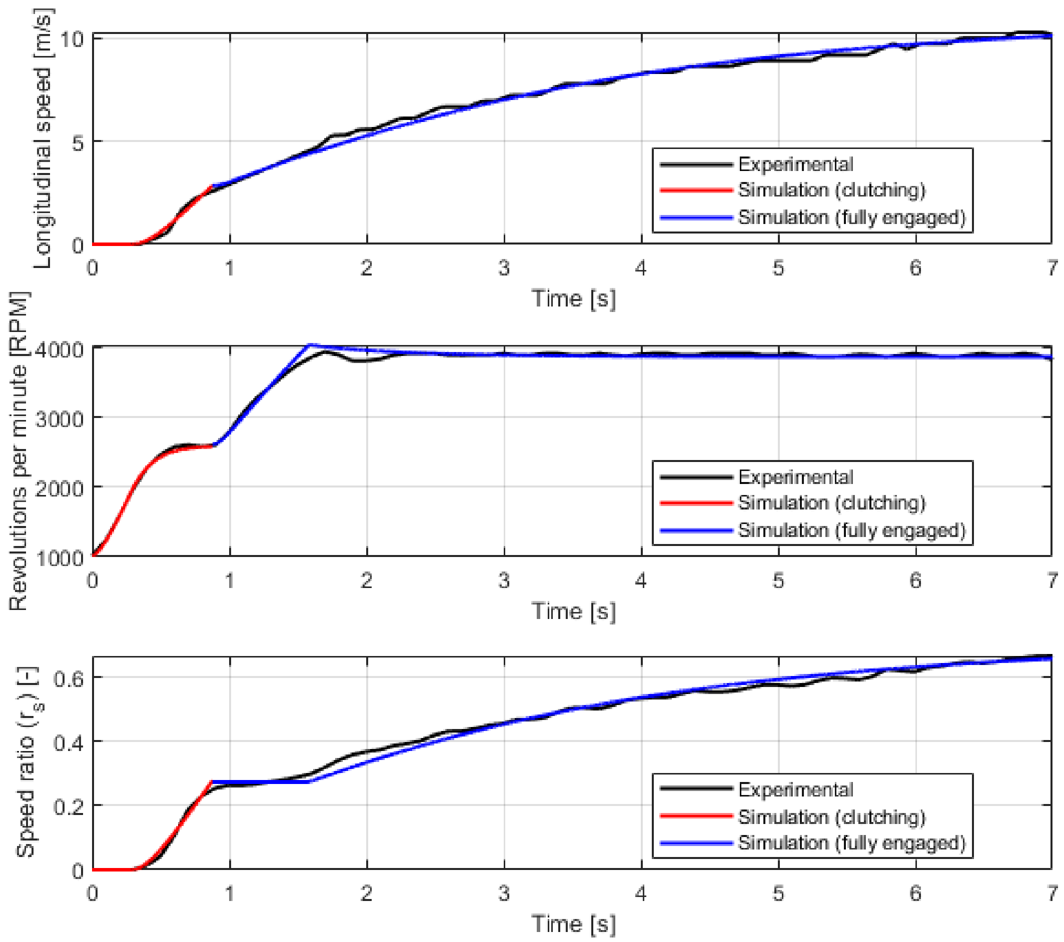

Figure 7 – Experimental and simulation results. The speed (top), RPM (middle), and speed ratio (bottom) graphs are presented for the experimental test (black) and the simulation environment in the clutching (red) and fully engaged (blue) phases.

5. DISCUSSION

The present experimental result does not represent the desirable performance concerning maximum acceleration. The chosen setup is only illustrative. The objective is only to demonstrate the model's ability to capture the system's core dynamics and adequately reproduce the impacts of the variation of the main parameters that characterize the vehicle.

The simulation results presented in this article show the ability of the proposed model to reproduce the experimentally performed acceleration. The main parameters of the model were previously measured. However, in some cases, the measurement uncertainties are high, and in other cases, the measurement was not carried out due to technical or financial impracticability. Therefore, the fine-tuning of the model was carried out through trial and error, in which some parameters were manually updated, within a reasonable range, to improve the fit of the simulated results on the experimental data.

After applying the throttle input, it is possible to observe that, for a brief period, the engine speed rises while the car remains at rest. The preload of the primary pulley determines the point at which the CVT transmission starts transmitting torque and puts the vehicle in motion by changing the engine RPM and the vehicle's longitudinal speed. For the setup used, it was observed that slippage occurs only on the primary pulley, as the preload on the secondary pulley is significantly higher. Therefore, the torque amplification between the two CVT pulleys does not exceed the slip limit between the belt and the secondary pulley sheaves.

The system is very sensitive to the ramp profile where the flyweight travels. The constant angle, equivalent to the variable angle present in the real CVT, was adjusted to promote the best fit in the experimental data, mainly in the shift-out phase. Although the CVT does not develop to a high ratio, the model can indicate the dependence of the ramp profile and the displacement stiffness of the sheaves in the extension of this phase. Sustaining constant RPM requires a specific tuning for this to occur.

6. CONCLUSIONS

This work presents the validation of a computational model of the longitudinal dynamics of a 2WD vehicle equipped with a flyweight-based CVT. The longitudinal speed and engine RPM signals from the computational environment adequately reproduce the experimental results of the real vehicle. The speed ratio signal has good adherence for most of the analyzed period. The mathematical model proposed in this document can serve as a basis for studying fuel economy and improving the dynamic performance of vehicles with this type of transmission.

Future work should address the improvement of the computational model. It must consider the friction limit in the tire-road interaction and the longitudinal load transfer. In addition, the CVT ramps must be implemented with a non-linear profile, like those used in the real vehicle. Finally, the precise measurement of the main parameters of the vehicle and the development of optimization frameworks for parametric identification should also be addressed.

7. REFERENCES

Aaen, O., 2015. Olav Aaen's Clutch Tuning Handbook: For Serious Racers and Anyone who Wants More Performance from Their Variable Ratio Belt-transmission.

Anderson, B., 2017. Analysis and Tuning of a Flyweight-Actuated Continuously Variable Transmission.

Arango, I. and Alzate, S.M., 2020. Numerical design method for CVT supported in standard variable speed rubber V-belts. Applied Sciences, 10(18), p.6238.

Aulakh, D.J.S., 2017. Development of simulation approach for CVT tuning using dual level genetic algorithm. Cogent Engineering, 4(1), p.1398299.

Bonsen, B., Klaassen, T.W.G.L., Van de Meerakker, K.G.O., Steinbuch, M. and Veenhuizen, P.A., 2003, January. Analysis of slip in a continuously variable transmission. In ASME International Mechanical Engineering Congress and Exposition (Vol. 37130, pp. 995-1000).

Bonsen, B., Pulles, R.J., Simons, S.W.H., Steinbuch, M. and Veenhuizen, P.A., 2005, August. Implementation of a slip controlled CVT in a production vehicle. In Proceedings of 2005 IEEE Conference on Control Applications, 2005. CCA 2005. (pp. 1212-1217). IEEE.

Ding, H.F., Zhu, C.C. and Liu, H.J., 2011. Influence of Flyweight Profile on Regulating Characteristic of Rubber V-Belt CVT. Applied Mechanics and Materials, 86, pp.210-213.

Gangadurai, M., Harikrishnan, N. and Sreekumar, B., 2005. Development of an Analytical Design Concept of Mechanically Controlled Continuously Variable Transmission (No. 2005-26-069). SAE Technical Paper.

Julió, G. and Plante, J.S., 2011. An experimentally-validated model of rubber-belt CVT mechanics. Mechanism and Machine Theory, 46(8), pp.1037-1053.

Khan, S.A. and Dhongde, S., 2014. Mathematical Modeling of Continuously Variable Transmission for Small Scooter Engine (No. 2014-01-2861). SAE Technical Paper.

Lolli, S., Cipollone, R., D'Amato, E. and Anatone, M., 2003. A theoretical and experimental procedure for design optimization of CVT belts. SAE transactions, pp.1069-1076.

Skinner, S.S., 2020. Modeling and Tuning of CVT Systems for SAE® Baja Vehicles. West Virginia University.

Srivastava, N. and Haque, I., 2009. A review on belt and chain continuously variable transmissions (CVT): Dynamics and control. Mechanism and machine theory, 44(1), pp.19-41.

Willis, C.R., 2006. A kinematic analysis and design of a continuously variable transmission (Doctoral dissertation, Virginia Tech).